ELSEVIER

Polymer 43 (2002) 4167–4176

polymer

www.elsevier.com/locate/polymer

Viscoelastic and mechanical properties of vinyl ester (VE)/multifunctional polyhedral oligomeric silsesquioxane (POSS) nanocomposites and multifunctional POSS–styrene copolymers

G.Z. Li[a], L. Wang[a], H. Toghiani[b], T.L. Daulton[c], C.U. Pittman Jr.[a,*]

[a] *Department of Chemistry, Mississippi State University, Mississippi State, MS 39762, USA*
[b] *Department of Chemical Engineering, Mississippi State University, Mississippi State, MS 39762, USA*
[c] *Naval Research Laboratory, Marine Geosciences Division, Stennis Space Center, MS 39529-5004, USA*

Received 20 December 2001; received in revised form 15 March 2002; accepted 21 March 2002

Abstract

Vinyl ester (VE) composites containing chemically bonded, multifunctional polyhedral oligomeric silsesquioxane (POSS), POSS-**1** ($(C_6H_5CHCHO)_4(Si_8O_{12})(CH{=}CHC_6H_5)_4$), nanoparticles were prepared with VE/POSS-**1** 95/5 and 90/10 w/w ratios. The mole percents of POSS-**1** in these two composites are low (<0.5 and $<1\%$, respectively) due to the high mass of POSS-**1** (mwt = 1305). VE composites of two non-functional POSS-**3** (octaisobutyl POSS) and POSS-**4** (dodecaphenyl POSS) derivatives were also prepared with 95/5 w/w compositions. Additionally, POSS-**1** was also incorporated into styrene copolymers at levels of 5 wt% (0.42 mol%) and 10 wt% (0.88 mol%) of POSS-**1**. The composites and copolymers were characterized by dynamic mechanical thermal analysis and mechanical testing. The POSS-**1** units incorporated into the vinyl ester network were well dispersed. No phase-separation in the VE/POSS-**1** 90/10 composite could be detected by TEM from low to 8×10^5 magnification. In VE composites containing 10 wt% POSS-**1**, silicon-rich phases were observed ranging in size from a few nm to ~75 nm by electron energy loss spectroscopy (EELS). TEM, EDXS, EELS and extraction studies suggest that some POSS-**1**-rich nanoparticles in the VE/POSS-**1** 90/10 composite are present and also a fraction of the POSS-**1** is molecularly dispersed within the VE resin. The POSS-**1**-rich dispersed phase portion is cross-linked, insoluble and contains some VE. VE/POSS-**3** and VE/POSS-**4** composites exhibited larger-sized POSS phases which do not contain VE. Incorporating low mole percentages of POSS-**1** into the VE network by chemical bonds or blending non-functional POSS-**3** or **4** into VE resin have almost no influence on T_g or on the width of the tan δ peak in the glass transition range. POSS-**1**–styrene copolymers exhibit good miscibility at 5 wt% POSS-**1** but serious phase-separation occurs in the copolymer with 10 wt% POSS-**1** content. POSS-**1**–styrene copolymers swelled but did not dissolve in tetrahydrofuran (THF) demonstrating they had been cross-linked by POSS-**1**. No POSS-**1** was extracted into the THF. The POSS-**1**–styrene copolymers have higher T_g values versus pure polystyrene (PS) prepared at the same conditions. The T_g elevation could be due to the cross-linking resulting from the four β-substituted styryl functions in POSS-**1** and due to the effect of high molecular weight POSS units retarding segmental motion of a portion of the chain segments. The T_g of the 10 wt% POSS-**1** copolymer is almost the same as that of the 5 wt% POSS-**1** copolymer because the continuous phase in the 10 wt% POSS-**1** copolymer might have a cross-linking density similar to that of the 5 wt% POSS-**1** copolymer. The low POSS-**1** mole percentage means that many all-styrene segments exist that can undergo segmental motion without being retarded by POSS. The tan δ peak for 10 wt% POSS-**1** copolymer is much broader and less intense than that for PS or 5 wt% POSS-**1** copolymer. A higher average cross-linking density and much less segmental motion in the dispersed POSS-**1**-rich phase account for this behavior in the 10 wt% copolymer. The bending storage modulus, E', values of the VE/POSS-**1** composites and the POSS-**1**–styrene copolymers are higher than those of either the neat vinyl ester resin or pure PS, respectively, over entire temperature range, especially at the low POSS-**1** content (5 wt%). The incorporation of multifunctional POSS-**1** into vinyl ester or PS by chemical bonding improves the thermal dimensional stabilities. The flexural modulus of the vinyl ester resin is raised by incorporation of POSS-**1** while the flexural strengths are lowered. VE resin and VE/POSS-**1** composites gave negligible weight gains after 50 days in toluene. The VE and composite samples cracked and fragmented after submersion in THF. © 2002 Published by Elsevier Science Ltd.

Keywords: Viscoelastic property; Mechanical property; Multifunctional polyhedral oligomeric silsesquioxane/vinyl ester nanocomposite

1. Introduction

The development of polymer–inorganic nanocomposites with improved properties has attracted much research

---

* Corresponding author. Tel.: +1-601-325-7616; fax: +1-601-325-7611.
E-mail address: cpittman@ra.msstate.edu (C.U. Pittman Jr.).

0032-3861/02/$ - see front matter © 2002 Published by Elsevier Science Ltd.
PII: S0032-3861(02)00232-X

interest in the past few years [1–10]. Polyhedral oligomeric silsesquioxane (POSS) reagents offer a unique opportunity for preparing hybrid organic–inorganic materials with the inorganic phase truly molecularly dispersed within the nanocomposites [11–15]. They combine a hybrid inorganic–organic composition, $R_n(SiO_{1.5})_n$, with nanosized cage structures having dimensions comparable to those of most polymeric segments or coils. POSS chemical reagents can be thought of as the smallest particles of silica possible. However, unlike silica, silicones or fillers, each POSS molecule contains either non-reactive or reactive organic substituents at the corner silicon atoms. These organic functions make the POSS nanostructure compatible with polymers or monomers. POSS derivatives are now available with reactive functionalities suitable for polymerization or grafting [1–15]. Hence, POSS nanostructured chemicals are easily incorporated using standard chemical methods into common plastics via copolymerization, grafting or blending [16,18,19].

The incorporation of POSS cages into polymeric materials often results in dramatic improvements in polymer properties, including increases in use temperature, oxidation resistance, and surface hardening, resulting in improved mechanical properties, as well as reductions in flammability and heat evolution. These enhancements have been shown to apply to a wide range of thermoplastic and a few thermoset systems, i.e. methacrylates [1], styrenes [2,3], norbornenes [5,20], ethylenes [21] and epoxies [4], siloxanes [17], etc. Therefore, many nanocomposites using functionalized POSS derivatives with traditional plastics and resins may be designed. For example, the monofunctional epoxy-substituted POSS monomer, $[(c\text{-}C_6H_{11})_7Si_8O_{12}(CH_2\overline{CHCH_2O})]$, **2**, was incorporated into a network composed of two difunctional epoxy monomers, the diglycidyl ether of bisphenol-A (DGEBA) and 1,4-butanediol diglycidyl ether (BDGE), at a DGEBA/BDGE 9/1 mole ratio [4]. The diamine-terminated poly(propylene oxide), Jeffamine D230 (with 38 propylene oxides and a molecular weight of 2248), was employed as the curing agent in an amount which gave a 1:1 equivalent of epoxy to amine functions [4]. The glass transition region was observed by DSC to broaden with an increase in weight percent of the POSS-**2** (≤10 wt%) but there was no change on the onset temperature of glass transition range [4]. The topological constraints provided by the presence of POSS-**2** reinforcements slowed the motion of the network junctions. Therefore, the time needed to reach structural equilibrium dramatically increased relative to that for non-nanoreinforced networks [4].

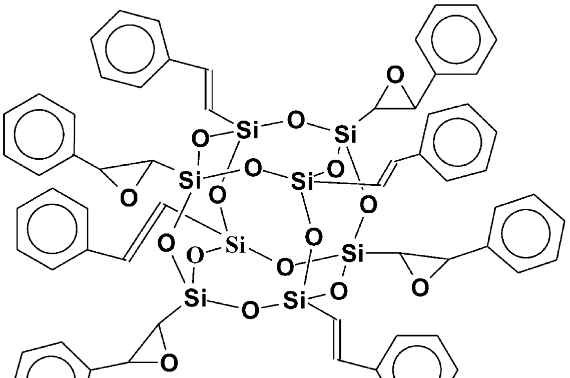

1

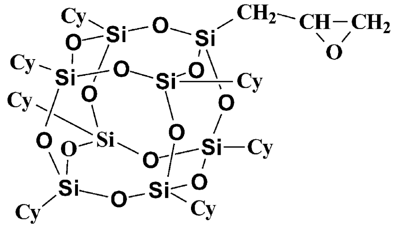

2

Cy = Cyclohexyl

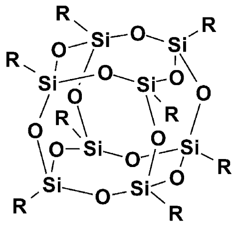

R=i-Butyl
3

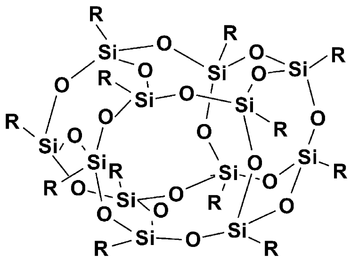

R=Phenyl
4

Very little research has appeared on the use of multifunctional POSS monomers in thermoset systems. We incorporated the multifunctional POSS-**1** into an aliphatic, low viscosity epoxy network and studied its viscoelastic properties (dynamic mechanical thermal analysis) and flexural moduli and strengths (stress–strain) [22]. We are unaware of any reports concerning the incorporation of mono- or multifunctional POSS into vinyl ester resins.

The monofunctional styryl–POSS monomers, $[(c\text{-}C_6H_{11})_7(Si_8O_{12})(CH_2CH_2C_6H_4CH{=}CH_2)]$ and $[(c\text{-}C_5H_9)_7(Si_8O_{12})(CH_2CH_2C_6H_4CH{=}CH_2)]$, were used to modify poly(methyl styrene) by copolymerization with methyl styrene [2,3]. When these copolymers contained 1 mol% of the styryl–POSS monomer, their T_g values were lower than that of poly(methyl styrene). As the styryl–POSS content increased to 9 mol%, the T_g values for copolymers became higher than that of pure poly(methyl styrene) and the T_g values increased steadily with a further increase in styryl–POSS content [2]. The incorporation of both these monofunctional styryl–POSS monomers into poly(methyl styrene) also improved the thermal stability, except for the modification in T_g at low POSS mole percents. The incorporation of either of these two styryl–POSS monomers into poly(methyl styrene) retarded greatly polymer chain segmental motion due to their high masses and large volumes. The viscoelastic behavior of these copolymers was modified as the POSS mole fraction increased to

8 mol%, resulting in a rubber-like behavior at high temperature [3]. However, no reports have appeared on modifications of polystyrene (PS) by multifunctional POSS derivatives such as POSS-**1**.

In this paper, multifunctional POSS-**1**, $[(C_6H_5CHCHO)_4(Si_8O_{12})(CH{=}CHC_6H_5)_4]$, with eight functional groups, including four β-substituted styrenes and four epoxidized styrenes, was blended with vinyl ester (VE) resin (containing 50 wt% styrene) and cured. VE/POSS-**1** composites with compositions of 95/5 and 90/10 w/w were prepared. Two VE composites containing the non-functional POSS derivatives, octaisobutyl POSS (POSS-**3**) and dodecaphenyl POSS (POSS-**4**), were also prepared. In addition, POSS-**1**–styrene copolymers with compositions of 5/95 and 10/90 w/w were made to see the effect of introducing low cross-linking densities by multifunctional POSS-**1**. Viscoelastic and mechanical properties of these VE/POSS composites and POSS-**1**–styrene copolymers were studied.

2. Experimental section

2.1. POSS-1 characterization and specimen preparation

Multifunctional POSS-**1**, $[(C_6H_5CHCHO)_4(Si_8O_{12})(CH{=}CHC_6H_5)_4]$, with eight functional groups including four epoxidized styrenes and four styrenes, was synthesized by R. Blanski, Air Force Research Laboratory, Edwards AFB and provided to us. A mixture of isomers is present but the ^{1}H NMR spectrum was still quite sharp with the exception of the epoxy ring hydrogens where broadening prevented a good measurement of the J value. Its chemical structure has been demonstrated by ^{1}H NMR (($CDCl_3$): δ 2.52 (1H, epoxy ring adjacent to Si), δ 4.06 (1H, epoxy ring adjacent to phenyl), δ 6.27 (1H, $J = 19$ Hz, vinyl proton adjacent to Si) and δ 7.35 (11H, $J = 19$ Hz 1H due to vinyl proton adjacent to phenyl group and 10H from the two types of phenyl rings)). The IR spectrum of POSS-**1** exhibited a strong wide absorption peak around 1102 cm^{-1}, due to the (Si_8O_{12}) cage, a weak sharp peak at 993 cm^{-1} due to the *trans* vinyl hydrogens' out-of-plane deformation and two peaks at 736 and 696 cm^{-1} due to monosubstituted phenyl ring out-of-plane hydrogen bending. Octaisobutyl POSS (POSS-**3**) and dodecaphenyl POSS (POSS-**4**) were purchased from Hybrid™ Plastics Co. The commercial vinyl ester resin, DERAKANE™ 510C-350, containing 35 wt% styrene, was purchased from Dow Chemical Co. Methyl ethyl ketone peroxide (MEKP) and Cobalt naphthanate (CoNap) were employed as the initiator/catalyst system to cure the resins.

POSS-**1** (0.684 or 1.444 g) was dissolved into styrene (3 g) to produce a transparent solution. This solution was mixed with the VE resin (10 g) to produce a clear transparent solution containing 50 wt% styrene. Then, 1 wt% MEKP and 0.2 wt% CoNap were added into this solution. This formulation was put into a mold without degassing, cured at room temperature for 24 h and postcured in an oven at 90 °C for 24 h followed by 150 °C for 5 h. VE/POSS-**3** and VE/POSS-**4** composites (see structures **3** and **4**) with 95/5 w/w compositions, were prepared employing the same conditions used for VE/POSS-**1**. A reference vinyl ester resin was also made by adding addtional styrene to DERAKANE™ 510C-350 to bring the styrene weight percentage to 50% and then this resin was cured using the same protocol. The reference VE resin, VE(50 wt% styrene)/POSS-**1** 95/5 and 90/10, VE/POSS-**3** 95/5 and VE/POSS-**4** 95/5 specimens were made in 69 mm × 38 mm × 3–4 mm sizes.

Styrene was purchased from Aldrich Chemical Company Inc. Methyl ethyl ketone peroxide and cobalt naphthanate were used as the initiating system for PS synthesis and for the copolymerization of styrene with POSS-**1**. POSS-**1** was weighed into styrene in specific amounts providing transparent styrene solutions. MEKP (0.5 wt%) and CoNap (0.1 wt%) were mixed into the styrene/POSS-**1** solutions. These solutions were placed in molds and cured at 85–88 °C in air for 3 days. The cured specimens were postcured at 90 °C for 24 h and then 120 °C for 5 h. POSS-**1**/styrene copolymers with compositions of 5/95 and 10/90 w/w were prepared. The out-of-plane hydrogen deformation band of POSS-**1** due to the *trans* double bond had largely disappeared relative to the 1102 cm^{-1} band of the Si_8O_{12} cage, indicating a high fraction of these bonds had been used in forming the resin. Pure PS samples were also produced at the same conditions used for making the copolymers. The pure PS sample exhibited molecular weight averages of $M_z = 1.58 \times 10^5$, $M_w = 1.00 \times 10^5$ and $M_n = 4.5 \times 10^4$ and a polydispersity of 2.22, measured using gel permeation chromatography (GPC) equipped with a light scattering detector. The solvent was tetrahydrofuran (THF). PS and the 5 wt% POSS-**1** copolymer were both transparent. In contrast, the 10 wt% POSS-**1** copolymer was opaque.

2.2. Measurements

The dynamic storage modulus E' and loss factor (tan δ) were determined in the bending mode using a Polymer Laboratories DMTA MK3 instrument. A dual-level bending mode was employed. Small amplitude bending oscillations (both 1 and 10 Hz) were used at a gap setting of 8.00 mm. The measurements were carried out from 30–45 to 180 °C for VE/POSS-**1** composites and from 35 to 115–140 °C for POSS-**1**/styrene copolymers. The temperature was raised at a rate of 2 °C min^{-1}. VE/POSS-**1** composite test samples were approximately 3.0–4.0 mm thick, 4.5–5.5 mm wide and 38 mm long. The PS and POSS-**1**/styrene copolymer samples were 40 mm × 6–7 mm × 2–2.5 mm.

Flexural strengths and flexural moduli of VE/POSS-**1** composites were determined according to ASTM D-790-92 using a Zwick Materials Testing Machine (1435). The specimens sizes employed were 38 mm (length) × 10 mm (width) × 3–4 mm (thickness). The flexural strength (FS) is defined (ASTM D790-92) as the strength when the specimen fails in the three point bending test and is calculated according to Eq. (1):

$$\mathrm{FS} = \frac{3PL}{2Wt^2} \tag{1}$$

where P is the breaking force of the specimen, L the support span, W the width, and t the thickness. The flexural modulus (FM) is calculated from the tangent to the steepest initial straight-line portion of the load–deflection curve and using Eq. (2):

$$\mathrm{FM} = \frac{L^3M}{4Wt^3} \tag{2}$$

where L is the support span, M the tangent of the initial straight-line portion of the load–deflection curve, W the width, and t the thickness.

A JEOL JEM-3010 analytical transmission electron microscope (JEOL USA Inc.), operating at 300 keV with a $\mathrm{LaB_6}$ filament and a measured point-to-point resolution of 0.21 nm, was used to characterize the phase morphology in the VE/POSS-**1** 90/10, VE/POSS-**3** 95/5, and VE/POSS-**4** 95/5 composites. Because VE/POSS-**1** 95/5 and 90/10 composites are transparent and the 90/10 sample contains more POSS, the VE/POSS-**1** 90/10 sample was selected for TEM measurements. Samples for TEM measurements were ultramicrotomed to ~60–80 nm thickness and mounted on holey amorphous-C coated Cu TEM grids. The JEM-3010 instrument was equipped with a side-entry motorized five axes goniometer, an energy dispersive X-ray spectroscopy (EDXS) system, and a Gatan imaging filter (GIF200) capable of electron energy loss spectroscopy (EELS). EDXS spot analysis of small POSS particles (phases) for Si and Br were done by condensing the beam to ~100 nm and collecting data for 2000 s, making frequent adjustments to compensate for specimen drift. Matrix spectra were obtained in the same manner, except no compensation for specimen drift was required. Long acquisition times and high probe current densities were required because the bromine concentration in the VE was below several weight percentage. The beam size could be reduced to smaller sizes (10 nm). EELS was used to analyze Si and C distributions in VE/POSS-**1** 90/10 sample.

3. Results and discussion

3.1. Vinyl ester/POSS composites: DMTA swelling and extraction studies

The bending storage modulus E' versus temperature curves at 1 Hz (from DMTA) for the neat vinyl ester and its VE/multifunctional POSS-**1** composites are shown in Fig. 1. Fig. 1 clearly shows that the E' values of VE/POSS-**1** 95/5 and 90/10 composites are higher than those of the neat VE resin. The E' values of the 90/10 composite are lower than those of the 95/5 composite at $T < T_g$. For an example, the E' values of neat VE, VE/POSS-**1** 95/5 and 90/10 composites at 40 °C are 1242, 1960, and 1584 MPa, respectively. In the rubbery region ($T > T_g$), the E' values of VE/POSS-**1** 95/5 and 90/10 composites are also higher than those of the neat VE resin. Furthermore, they increase with the POSS content. The E' values of neat VE, VE/POSS-**1** 95/5 and 90/10 at 160 °C are 8.30, 9.02, and 10.47 MPa, respectively. Thus, E' values for these composites are higher than those of the neat VE resin over the entire temperature range and these composites have higher thermal dimensional stabilities than that of the neat VE resin.

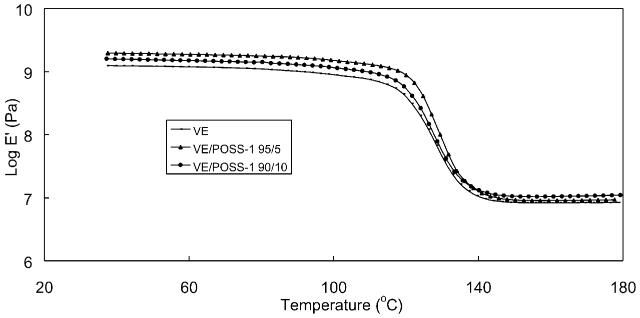

Fig. 1. Bending modulus (E') versus temperature curves at 1 Hz (from DMTA) for neat VE and its VE/POSS-**1** 95/5 and 90/10 w/w composites.

Fig. 2 shows the bending tan δ versus temperature curves at 1 Hz (from DMTA) for the VE resin and the VE/POSS-**1** composites. The incorporation of multifunctional POSS-**1** into VE has almost no influence on the width of tan δ peak in glass transition range. The VE/POSS-**1** 90/10 composite exhibits a less intense tan δ peak than either the neat VE resin or the 95/5 composite. The glass transition temperature (T_g) is defined, herein, as the tan δ peak temperature. The T_g values of the neat VE resin and VE/POSS-**1** 95/5 and 90/10 composites are 130.6, 131.8, and 131.1 °C, respectively. Thus, given some experimental variations, the inclusion of multifunctional POSS-**1** into the VE had no measurable effect on T_g.

The VE resin contains 50 wt% styrene monomer and we have demonstrated that cross-linking does occur between

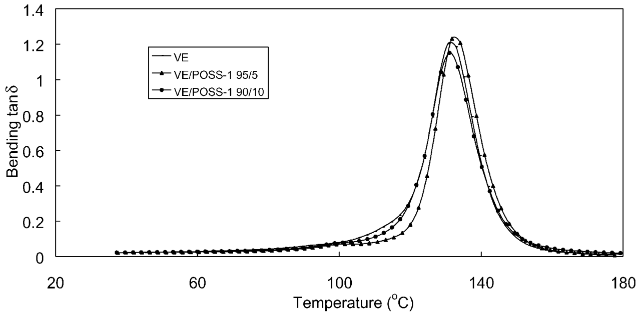

Fig. 2. Bending tan δ versus temperature curves at 1 Hz (from DMTA) for neat VE and its VE/POSS-**1** 95/5 and 90/10 w/w composites.

styrene and POSS-**1** (discussed in Section 3.2). There is no question that the styrenic double bonds of POSS-**1** undergo reaction with the developing vinyl ester resin as it cures. The out-of-plane deformation band at 993 cm^{-1}, due to the *trans* vinyl hydrogens of POSS-**1** monomer, disappeared in IR spectra of the VE/POSS-**1** composites. Thus, POSS-**1** is chemically bonded to the network of VE. However, the 993 cm^{-1} band is partially superimposed on the wide, 1102 cm^{-1} Si–O absorption band, so it is impossible to tell if all the styrenic groups in POSS-**1** were consumed.

The styrenic double bonds in POSS-**1** are disubstituted with a large phenyl ring on one carbon and an extremely bulky corner $-(SiO_{1.5})_8-$POSS cage on the other carbon. Thus, the radical addition to the double bond of POSS-**1** by growing methacryl or styryl radicals and propagation of the resulting radicals during cure might be slower than those same reactions on styrene or the methacrylate functions in the VE. Incorporation of POSS-**1** into the resin's network might be slower than the other VE monomers. During curing, if the styrene groups in POSS-**1** were less reactive than those in the vinyl ester resin components, all four of the substituted styryl functions of POSS-**1** might not always react in cross-linking. Importantly, the high molecular weight of POSS-**1** (1305) means its mole percent is quite low in the resin. As a result, the incorporation of a small amount of multifunctional POSS-**1** ($\leq$10 wt%) into the VE might have less influence on the cross-linking density in the resulting VE/POSS-**1** composites. Therefore, VE/POSS-**1** composites exhibit almost the same T_g as that of the neat VE resin.

The neat VE resin and the VE/POSS-**1** 95/5 composite were submerged in toluene at room temperature (22–25 °C) for 50 days to study their swelling behavior. After removal from solvent there was almost no weight increase observed due to imbibed solvent (0.16% for VE and 0.67% for the VE/POSS-**1** 95/5 composite). When the two samples were submerged in THF at room temperature for 12 h or more, cracks appeared in both two samples and they fragmented into many small pieces. The cracks formed and propagated more rapidly in the 95/5 composite than in the neat VE resin. Thus, it was not possible to characterize the cross-linking density of either the neat VE resin or the VE/POSS-**1** composites by solvent swelling studies. Although THF is a good solvent for VE precursor and POSS-**1** monomer, no POSS-**1** could be extracted after VE/POSS-**1** composite was submerged in excess THF for 50 days and highly fragmented. Therefore, POSS-**1** was incorporated into VE network by chemical bonding and could not be leached or extracted.

POSS-**1** moieties incorporated into the VE network will retard segmental motion due to their high mass and large volume. The large volume of the POSS-**1** moiety requires a large void volume to move into as it changes location during segmental motion. It is difficult for this moiety to move through a volume of resin containing other polymer chains. The large mass also resists rapid translocation. Attaching a POSS moiety to a polymer chain segment is somewhat like attaching an anchor to a jump rope. Even at high temperature ($>T_g$), the motion of segments with POSS-**1** bound by only one chemical bond will experience restrictions. This could account for the higher E' values of the VE/POSS-**1** 95/5 and 90/10 composites over the entire temperature range. This does not explain why the VE/POSS-**1** 90/10 composite displays lower E' values, at $T < T_g$, than the 95/5 composite. Perhaps, the glassy state of the 90/10 composite has a slightly larger free volume versus that of the 95/5 composite due to the higher POSS loading in the former. This might lower the values of E' in the glassy region.

In addition to making VE/POSS-**1** composites, vinyl ester composites with two other POSS derivatives, octaisobutyl POSS (POSS-**3**) and dodecaphenyl POSS (POSS-**4**), were made. The latter has a $Si_{12}O_{18}$ core, which is bigger than the Si_8O_{12} cores of POSS-**1** and POSS-**3**. These two POSS molecules can be designated as molecular silicas. They have no polymerizable functions. Hence, they cannot chemically bond to components of the VE resin matrix. Furthermore, neither could be dissolved completely in styrene. Thus, after mixing with the monomer precursors of the VE resin followed by curing, phase-separation in both VE/POSS-**3** 95/5 and VE/POSS-**4** 95/5 composites was clearly observed. The VE/POSS-**3** 95/5 composite is opaque while the VE/POSS-**4** composite is translucent. Some POSS particles in both composites were quite large. The POSS particles present in the VE/POSS-**4** composite, observed by unaided eye, are smaller than those in the VE/POSS-**3** composite.

These observations contrasted sharply with the VE/POSS-**1** systems. POSS-**1** easily dissolved into styrene and formed transparent solutions. After blending these solutions with the VE resin precursors, no phase-separation was observed. During curing, POSS-**1** molecules react with propagating radical chains and become part of the growing polymer. Furthermore, POSS-**1** participates in the cross-linking due to its multifunctionality. Thus, as VE monomers are consumed, POSS-**1** becomes immobilized as part of the growing VE network. Even if its solubility limit was reached during the cure process, the bound POSS-**1** may be unable to phase separate or aggregate with only a few POSS moieties. Thus, the VE/POSS-**1** composites display good transparency. However, nanometer-sized POSS-**1**-rich regions (<80 nm) were observed in the VE/POSS-**1** 90/10 composite and this will be discussed later.

DMTA curves of VE/POSS-**3** 95/5 and VE/POSS-**4** 95/5 composites shown in Figs. 3 and 4 have been measured at the same conditions applied to the VE resin and the VE/POSS-**1** 95/5 composite. The T_g values of VE, VE/POSS-**1** 95/5, VE/POSS-**3** 95/5 and VE/POSS-**4** 95/5 composites (Fig. 4) are 130.6, 131.8, 132.1, and 130.6 °C, respectively. Under the given experimental variations, no appreciable difference among their T_g values is apparent.

The E' values at 40 °C ($<T_g$) of VE/POSS-**3** 95/5 and VE/POSS-**4** 95/5 composites (Fig. 3) are 1153 and 1353 MPa. These values are much lower than that (1960 MPa) of

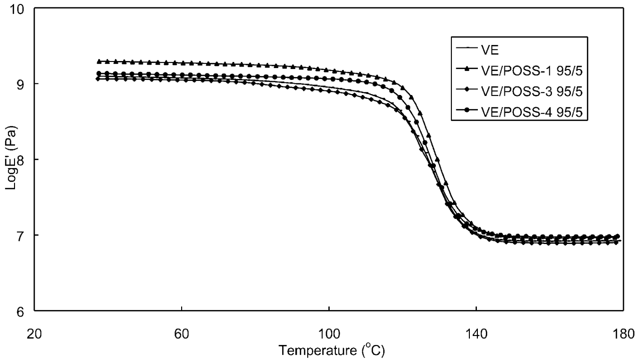

Fig. 3. Bending modulus (E') versus temperature curves at 1 Hz (from DMTA) for neat VE resin and its VE/POSS-**1**, VE/POSS-**3**, and VE/POSS-**4** composites.

VE/POSS-**1** 95/5 composite (Fig. 3). The composites of VE with POSS-**1** and POSS-**4** both exhibit higher E' values than that of the neat VE resin (1242 MPa). At 160 °C ($>T_g$), the E' values of VE/POSS-**3** and VE/POSS-**4** composites are 7.78 and 9.48 MPa, respectively. The neat VE resin (8.30 MPa) and VE/POSS-**1** 95/5 composite (9.02 MPa) both exhibit lower E' values than VE/POSS-**4** composite at temperatures above T_g (160 °C). The VE/POSS-**3** composite displays lower E' values than those of VE and VE/POSS-**1** composites. The phenyl rings on the outer periphery of POSS-**4** units may interact favorably with the abundant phenyl rings in the VE resin, inhibiting segmental motion of the VE network and increasing the E' values of the VE/POSS-**4** composite. The VE/multifunctional POSS-**1** composite exhibits higher E' values than the VE resin or the VE/POSS-**3** composite over the entire DMTA scan temperature range, suggesting that the incorporation of multifunctional POSS-**1** into VE networks by chemical bonding improves the E' values.

The flexural strengths and moduli of VE and VE/POSS composites are shown in Table 1. The flexural strengths of VE/POSS-**1** 95/5 and 90/10 composites are substantially lower than that of neat VE, but their flexural moduli are higher. These moduli increase with an increase POSS-**1** content. Moreover, the bending deformation values at the maximum force of the composites are slightly smaller than that of the neat VE resin and decrease with increase in POSS-**1** content. In contrast, VE/POSS-**3** and VE/POSS-**4**, exhibit lower moduli at room temperature than those of the VE/POSS-**1** composites and the neat VE resin. Also, their strengths and bending deformations are much lower than those of both the VE resin and the VE/POSS-**1** composites. Thus, the incorporation of multifunctional POSS-**1** by chemical bonding improves the mechanical properties of VE resins versus the use of non-functional POSS derivatives **3** and **4**. The vinyl ester becomes much stiffer and slightly more brittle upon incorporation of POSS-**1**.

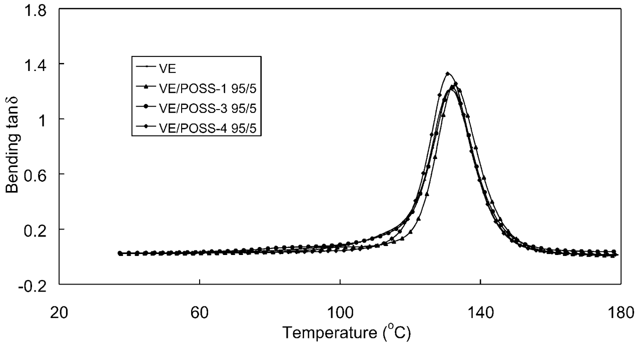

Fig. 4. Bending tan δ versus temperature curves at 1 Hz (from DMTA) for neat VE and its VE/POSS-**1**, VE/POSS-**3**, and VE/POSS-**4** composites.

Table 1
Flexural strengths (FS) and flexural moduli (FM) of neat VE and its VE/POSS composites

Samples	FS (MPa)	FM (MPa)	*L* at *F*-max (mm)
VE	191.85	1892.88	1.45
VE/POSS-**1** 95/5	174.56	1925.95	1.17
VE/POSS-**1** 90/10	151.68	2144.67	1.07
VE/POSS-**3** 95/5	65.39	1534.90	0.63
VE/POSS-**4** 95/5	66.03	1594.55	0.67

3.2. VE/POSS composites: TEM, EDXS and EELS studies

Transmission electron microscopy (TEM) was used to identify and characterize any phase-separation in these VE/POSS composites. We have previously observed polyphenylsilsesquioxane (PPSQ) particles exhibiting high contrast, with diameters of several micrometers, dispersed in continuous polycarbonate (PC) matrices by TEM [23]. The empirical formula, $[SiO_{1.5}]$, for the core of POSS, is the same as that of PPSQ ladder-like double chains. In this work, composites containing POSS-**3** or POSS-**4** with no polymerizable functions exhibited phase-separation. The VE/POSS-**3** 95/5 composite is opaque and has macroscopic POSS-**3** aggregated particles with a broad size distribution (<10–300 μm) and irregular shape, which are visible by the unaided eye. Some small POSS-**3** particles with sizes less than 1 μm, were observed by TEM. In comparison, the VE/POSS-**4** 95/5 composite is translucent and particles of about 100 μm diameters with faceted rectangular morphology were present. Smaller irregular POSS-**4** particles (30 μm) were observed by TEM. EDXS studies showed predominately Si, with only a little Br, was present in these POSS-**3** or POSS-**4** submicron particles (Br is present in a fire retarding monomer which is a component of the VE resin matrix). More Br was seen in the EDXS spectra as the particle size decreased. This represents contributions from the matrix surrounding and, perhaps, infiltrating the particles. The Si/Br ratio was consistently greater than the surrounding matrix.

Good contrast between POSS aggregates and the VE matrix exists in TEM measurements. Therefore, POSS-**1** particles or aggregates should be observable in very small

Fig. 5. TEM micrograph of the VE/POSS-**1** 90/10 composite at 800 000 × magnification. (The area above the boundary is the 90/10 composite).

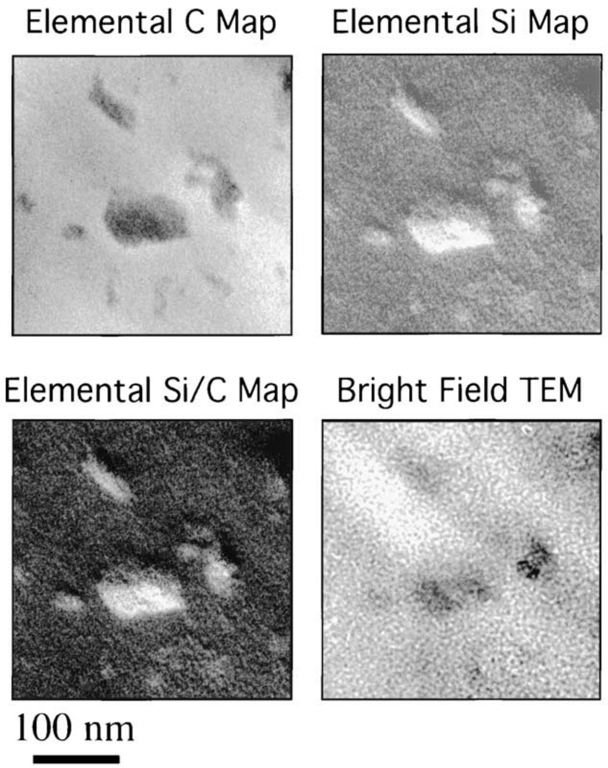

Fig. 6. Elemental C, Si and Si/C maps (from EELS) and brightfield TEM of the VE/POSS-**1** 90/10 composite.

particle sizes. However, TEM did not yield clear-cut evidence for such aggregates. No high contrast features were observed in the VE/POSS-**1** 90/10 composite at a TEM magnification of 8×10^5 (Fig. 5). Thus, the TEM contrast might be too low to observe very small POSS-**1** phases. However, nanometer-scale low contrast TEM features which might represent POSS-**1** aggregates were observed. They appear to be POSS-enriched regions containing some VE resin which lowers the contrast with the surrounding matrix region. They were examined by EDXS and found to have a slightly higher Si/Br ratio compared to the matrix. However, the EDXS measurements reported here have a resolution that is limited to the probe size and beam spreading. High probe currents were needed to detect the trace amounts of Br in the matrix, therefore probe diameters significantly below 100 nm could not be used with Br. GIF energy-filtered images have higher special resolution and showed that smaller low contrast features ($\leq$75 nm) were Si-rich and C-depleted with respect to the surrounding VE/POSS-**1** matrix (Fig. 6).

A series of energy-filtered images were collected on the VE/POSS-**1** 90/10 sample. EELS images were produced by allowing only electrons with a particular energy loss (within a 15 eV window) to contribute to the image. Two pre-adsorption edge images were used to model the background for subtraction from the postadsorption image. The absorption edges used to form elemental maps for C and Si were the 284 eV (C–K edge) and 99 eV (Si–L edge). Fig. 6 shows elemental C, Si, and Si/C maps for one representative location of VE/POSS-**1** 90/10 sample. Brighter contrast in the carbon map indicates higher values of C%. Likewise, brighter contrast in the Si map, indicates higher values of %Si. The relative intensity within an image is directly proportional to the concentration of the mapped elements. One can see clearly a few POSS-**1**-rich regions with sizes from ~75 nm to a few nm. Some POSS-**1** units are dispersed well in the matrix.

Small regions from 75 nm to a few nm in diameter were Si-rich and C-depleted relative to the surrounding matrix, but the surrounding areas also contained Si. The volumetric ratio of Si-rich/C-depleted particles was estimated from areal densities of particles present in GIF Si/C ratio maps. The dimension of the particle in the direction normal to the plane of the image was estimated from the projected particle diameter or 80 nm (the film thickness), whichever is smaller. The estimated volumetric ratio of these features was ≈2.5–5.5%. Since the densities of VE/POSS-**1** (1.218 g cm^{-3}) and VE (1.213 g cm^{-3}) are nearly the same, the volumetric ratio of POSS-**1** to VE in VE/POSS 90/10 is ≈10%. Hence, the estimated volumetric ratio from GIF Si/C maps suggests POSS-**1** units are distributed molecularly within the matrix. In further support, EELS and EDXS show the matrix regions also contain Si. Since pure VE contains no Si, the Si observed must be due to molecular level incorporation of POSS-**1** within the VE matrix structure. Thus, the best interpretation is that some POSS-**1** aggregation is taking place but other fractions of the POSS-**1** are distributed molecularly within the matrix. POSS-**1** has a diameter of about 0.6 nm. Each POSS-**1** core is surrounded by eight phenyl rings containing organic substituents. Many of these are chemically bonded to the VE matrix which is rich in styrene. Thus, the image contrast of single POSS-**1** moieties or even multinanometer clusters is low and difficult to detect. However, EELS does resolve differences in POSS-**1** distributions down to several nanometers.

The TEM/EDXS/EELS observations suggest that POSS-**1** is exceptionally well dispersed in the VE/POSS-**1** 90/10 sample. TEM demonstrates some POSS-**1**-rich phase regions ranging in size from a few nm to ~75 nm exist in the continuous VE/POSS-**1** phase. This continuous VE matrix phase also contains POSS-**1**. We do not know the extent of VE resin present within the dispersed POSS-**1**-rich phase or how it varies with the size of the phase. However, the inability to leach or extract POSS-**1** and the IR studies confirm that POSS-**1** units in both the Si-rich and Si-depleted phases are polymerized.

Two factors lead to this good dispersion of POSS-**1**. First, there is good miscibility between POSS-**1** and the VE precursors. POSS-**1** is soluble in the VE monomer mixture. Secondly, POSS-**1** is incorporated into the developing VE matrix by chemical bonding as that matrix forms. Hence, even if its solubility limit was reached during some point in the cure, POSS-**1**, when bonded to VE, is no longer free to aggregate. This limits the amount of phase-separation and only a few POSS-**1**-rich particles with small sizes (≤75 nm) were formed. These POSS-**1** rich particles also contain some VE resin. From earlier discussion, the VE/POSS-**1** composites belong to a class of nanocomposites in which multifunctional POSS units with a molecular weight of 1305 are well dispersed and chemically bonded within an organic matrix (VE resin) and some POSS-**1**-rich nanoparticles with sizes from a few nm to ~75 nm are also present. If the polymerizable functions on POSS-**1** had a higher polymerization reactivity, we would expect more POSS-**1** would bond to the developing matrix earlier in the polymerization. This should result in less phase-separation.

3.3. Multifunctional POSS–styrene copolymers

Polystyrene and POSS-**1**–styrene copolymers containing 5 and 10 wt% POSS-**1** were prepared under the same free radical initiation conditions. The PS samples were easily dissolved in THF solvent to form transparent solutions. However, neither of the POSS-**1**–styrene copolymers dissolved in THF. Instead, swelling of the copolymers in THF was observed. The copolymers formed gels showing that cross-linking had occurred. In addition, the IR absorption peak at 993 cm^{-1}, due to the *trans* vinyl hydrogens out-of-plane deformation of POSS-**1** monomer, disappeared in the POSS-**1**–styrene copolymers, indicating that most vinyl groups of the incorporated POSS-**1** had reacted with styrene. This cross-linking can only occur at POSS-**1** sites and these are present in very low mole percentages (0.42 and 0.88%, respectively, in the 5/95 and 10/90 composites). After swelling the copolymers in THF for 1 month, only uncross-linked PS molecules (45.02 wt% for the 5 wt% copolymer and 40.26 wt% for the 10 wt% copolymer) were extracted. No POSS-**1** was removed during these extractions. This demonstrates that many of the four β-substituted styrene functionalities in POSS-**1** reacted with growing polymer radicals under the mild conditions used. The volumes of the 5 wt% (0.42 mol%) and 10 wt% (0.88 mol%) POSS-**1**–styrene copolymers greatly increased after swelling in THF at room temperature for 1 day by 6.28- and 4.40-fold, respectively. The equilibrium swelling ratios of the 5 and 10 wt% POSS-**1**–styrene copolymers in toluene are 8.5 and 5.6, respectively, at room temperature. Thus, the average cross-linking density in the 10 wt% copolymer is higher than that in the 5 wt% copolymer. Furthermore, the shape of copolymer samples was almost the same after swelling as before swelling. These swelling factors may be compared to those of styrene–divinylbenzene copolymers in toluene. At divinylbenzene levels of 0.3 wt% (0.24 mol%), 0.5 wt% (0.40 mol%), 1.0 wt% (0.80 mol%) and 2.0 wt% (1.59 mol%), the volume swelling factors are 7, 5.5, 3.4, and 2.5, respectively.

The bending storage modulus E' versus temperature curves at 1 Hz (from DMTA) for PS and POSS-**1**–styrene copolymers containing 5 and 10 wt% of POSS-**1** are shown in Fig. 7. The E' values of these copolymers are substantially higher than those of pure PS over the entire temperature range. The copolymers display a rubbery plateau over a broader temperature range than pure PS sample prepared under identical conditions. The copolymers containing 5 wt% (0.42 mol%) and 10 wt% (0.88 mol%) of POSS-**1** exhibit bending storage moduli of 1717 and 1750 MPa, respectively, at 40 °C, versus 797 MPa for the PS. Thus, small amounts of incorporated POSS-**1** greatly modify the storage modulus and the thermal dimensional stability of the copolymers when prepared in an identical manner with the PS to which they are being compared.

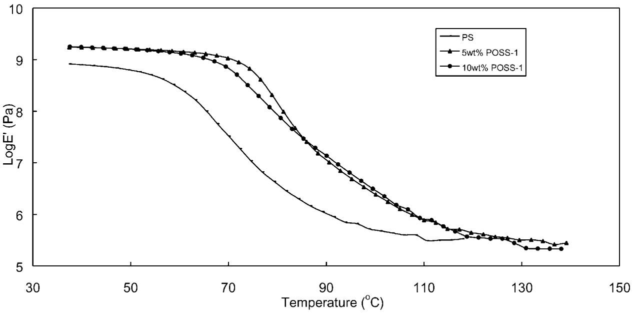

Fig. 7. Bending storage modulus (E') versus temperature curves at 1 Hz (from DMTA) for PS and the POSS-**1**–styrene coplymers containing 5 and 10 wt% POSS-**1**.

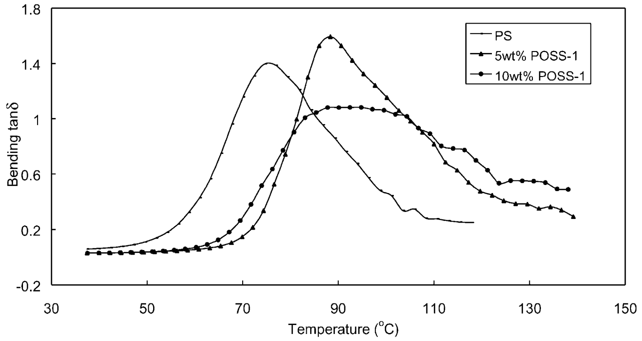

Fig. 8. Bending tan δ versus temperature curves at 1 Hz (from DMTA) for PS and the POSS-**1**–styrene compolymers containing 5 and 10 wt% POSS-**1**.

Fig. 7 shows the small difference between the E' values of the 5 and 10 wt% POSS-**1** copolymers. The copolymer with 10 wt% of POSS-**1** exhibits slightly lower E' values than the 5 wt% copolymer in some specific temperature ranges (50–80 and 115–140 °C). In contrast to PS, cross-linking did occur in the copolymer due to multifunctionality in POSS-**1**. The great increase in the storage modulus of the POSS-**1**–styrene copolymers is partially attributed to this cross-linking.

The bending tan δ versus temperature curves obtained at 1 Hz (from DMTA) for PS and the POSS-**1**–styrene copolymers are shown in Fig. 8. The T_g values, defined as the tan δ peak temperatures, are 70.9, 88.3, and 87.8 °C for PS and the 5 and 10 wt% POSS-**1** copolymers, respectively. PS showed a low T_g and a wide glass transition region compared with some commercial PS grades. This PS sample has a molecular weight distribution of $M_n = 4.51 \times 10^4$, $M_w = 1.00 \times 10^5$, $M_z = 1.58 \times 10^5$ and a broad distribution ($M_w/M_n = 2.22$). A low molecular weight fraction was present in the 2000–10 000 range which could act as plastizer and might lower the T_g. The higher T_g values for the POSS-**1**–styrene copolymers versus PS are, in part, attributed to the cross-linking by POSS-**1**. Furthermore, the pendant POSS units retard or restrict some segmental motion of PS. This latter effect has been demonstrated on uncross-linked poly(methyl styrene)/POSS systems as discussed earlier [2,3].

The 10 wt% POSS-**1**–styrene copolymer exhibits almost the same T_g as 5 wt% POSS-**1** copolymer. It has a lower onset temperature of the glass transition region and a less intense tan δ peak versus those of the 5 wt% copolymer. The copolymer T_g values are independent of the amount of POSS-**1** although the average cross-linking density of copolymer with 10 wt% POSS-**1** is slightly higher than that of 5 wt% POSS-**1** copolymer. The phase morphologies are different in the copolymers. PS and the copolymer containing 5 wt% POSS-**1** are both transparent while the 10 wt% POSS-**1** copolymer is opaque, indicating that major phase-separation has occurred only in the 10 wt% copolymer. Clear solutions of POSS-**1** and styrene were formed at room temperature to 85–88 °C prior to copolymerization. During the polymerization, however, phase-separation occurred in the 10 wt% sample but not in the 5 wt% sample. Thus, in the latter sample, all of the β-styryl functions of all the POSS-**1** present are eligible to react with styrene or growing polymer chains. This would result in good dispersion of cross-linking points throughout the 5 wt% POSS-**1** sample. Serious phase-separation during polymerization of the 10 wt% sample forms a dispersed POSS-**1**-rich phase and a PS-rich continuous phase. The dispersed POSS-**1**-rich phase might have a high cross-linking density and certainly has different properties from the continuous phase. The PS-rich continuous phase with a lower cross-linking density might be similar to the 5 wt% POSS-**1** sample. The continuous phase of the 10 wt% copolymer has almost same T_g as the 5 wt% copolymer. This might be the reason why the E' values of the 10 wt% copolymer are quite similar with those of the 5 wt% copolymer. Coexistence of the two phases may be the reason why the 10 wt% POSS copolymer has a wider tan δ peak than the 5 wt% copolymer. The slightly higher average cross-linking density and higher POSS-**1** loading might contribute to the less intense tan δ peak for the 10 wt% copolymer, while the low mole fractions of POSS-**1** incorporated into the two styrene copolymers does little to differentiate their T_g values.

In summary, the storage modulus and T_g of PS are improved by its copolymerization with POSS-**1** due to cross-linking in the copolymers and the restriction of segmental motion by attached POSS-**1** moieties. The 10 wt% POSS copolymer exhibits almost the same T_g and lower E' values at some temperatures versus those of the 5 wt% POSS copolymer. Serious phase-separation in the 10 wt% sample ultimately affects its DMTA response.

4. Conclusions

Multifunctional POSS-**1** was well dispersed after it was mixed with a commercial vinyl ester (50 wt% styrene) resin and cured. Significant dispersion was probably on the molecular scale, at POSS-**1** weight percents of 5 and 10%. TEM, EDXS, and EELS studies when combined show POSS-**1**-rich nanoparticles (~75 nm to a few nm) are present in the VE/POSS-**1** 90/10 composite. Furthermore, a portion of the POSS-**1** units are well dispersed in the matrix. In contrast, much larger sized phase-separation occurred when the non-functionalized ‘molecular silicas’, POSS-**3** and POSS-**4,** were blended into VE monomers and cured. The miscibility of the POSS-**1** units in its styrene copolymers is good only at low POSS-**1** contents (≤5 wt% or ≤0.42 mol%). Serious phase-separation is clearly observed as the POSS-**1** weight percent increased to 10%.

The incorporation of small amounts of POSS-**1** (≤10 wt%) into the vinyl ester network has almost no influence on T_g and the glass transition region. While POSS-**1** is massive and will reduce segmental motion of segments it is bound to, its mole percent is <1% in these systems. Therefore, it can only reduce segmental motion of a small fraction of the segments which contribute to the T_g. Also, VE resins are cross-linked without POSS-**1**, hence, addition of POSS-**1** may not raise the volume density of cross-links. Blends of POSS-**3** or **4** in VE also did not affect the T_g. In contrast, the T_g values of 5 and 10 wt% POSS-**1**–styrene copolymers are substantially higher than that of the pure uncross-linked PS due to the cross-linking induced by POSS-**1** and to the restriction of segmental motion by the massive and bulky POSS moieties. However, T_g of the 10 wt% POSS-**1** copolymer is almost same as that of the 5 wt% POSS-**1** copolymer because the continuous phase in the 10 wt% POSS-**1** copolymer might have a cross-linking density similar to that of the 5 wt% POSS-**1** copolymer.

The storage modulus, E', values of VE/POSS-**1** composites are higher than those of neat VE resin over the entire temperature range. The POSS-**1**–styrene copolymers exhibit higher E' values than pure PS. Therefore, thermal dimensional stabilities of vinyl ester or PS are increased by the incorporation of very low weight percents (and extremely low mole percents) of this multifunctional POSS. This trend is especially pronounced at low POSS-**1** content (5 wt%). The flexural modulus and hardness of vinyl ester resin is improved by incorporating POSS-**1** while its flexural strength is decreased by POSS-**1**. The flexural strength and moduli of VE/POSS-**3** 95/5 and VE/POSS-**4** 95/5 composites are smaller than those of neat VE. It is important to recognize that heat distortion temperatures and other properties can be sharply affected even when T_g does not change much upon chemically incorporating ~1 nm sized molecular phases. Swelling/extraction studies showed that POSS-**1** is chemically bonded to both the VE/POSS-**1** composites and the POSS-**1**–styrene copolymers.

Acknowledgements

This work was supported by a grant from the Air Force Office of Scientific Research (No. F49620-99-1-0191).

References

[1] Lichtenhan JD, Otonari YA, Carr MJ. Macromolecules 1995;28:8435.
[2] Haddad TS, Lichtenhan JD. Macromolecules 1996;29:7302.
[3] Romo-Uribe A, Mather PT, Haddad TS, Lichtenhan JD. J Polym Sci, Part B: Polym Phys 1998;36:1857.
[4] Lee A, Lichtenhan JD. Macromolecules 1998;31:4970.
[5] Mather PT, Jeon HG, Romo-Uribe A, Haddad TS, Lichtenhan JD. Macromolecules 1999;32(4):1194.
[6] Lee A, Lichtenhan JD. J Appl Polym Sci 1999;73:1993.
[7] Jeon HG, Mather PT, Haddad TS. Polym Int 2000;49:453.
[8] Fu BX, Hsiao BS, White H, Rafailovich M, Mather PT, Jeon PT, Jeon HG, Phillips S, Lichtenhan J, Schwab J. Polym Int 2000;49:437.
[9] Gonzalez RI, Phillips SH, Hoflund GB. J Space Rkts 2000;37(4):463.
[10] Ellsworth MW, Gin DL. Polym News 1999;24:331.
[11] Lichtenhan JD, Schwab JJ, Reinerth Sr. WA. Chem Innovat 2001;1:3.
[12] Mark JE, Lee CYC, Bianconi PA, editors. Hybrid organic–inorganic composites. ACS Symposium Series, vol. 585. 1995.
[13] Coltrain BK, Sanchez C, Schaefer DW, Wilkes GL, editors. Better ceramics through chemistry VII: organic/inorganic hybrid materials. MRS Symposium Proceedings, vol. 435. 1996.
[14] Laine RM, Sanchez C, Brinker CJ, Giannelis E, editors. Organic/inorganic hybrid materials. MRS Symposium Proceedings, vol. 519. 1998.
[15] Klein LC, Francis LF, De Guire MR, Mark JE, editors. Organic/inorganic hybrid materials II. MRS Symposium Proceedings, vol. 576. 1999.
[16] Haddad TS, Stapleton R, Jeon HG, Mather PT, Lichtenhan JD, Phillips S. Polym Prepr 1999;40(1):496.
[17] Haddad TS, Lee A, Phillips SH. Polym Prepr (ACS Div Polym Chem) 2001;42(1):88.
[18] Blanski RL, Phillips SH, Lee A. Polym Prepr (ACS Div Polym Chem) 2001;42(1):173.
[19] Tamaki R, Samura K, Chujo Y. Chem Commun 1998:1131.
[20] Bharadwaj BK, Berry RJ, Farmer BL. Polymer 2000;41:7209.
[21] Tsuchida A, Bolln C, Sernetz FG, Frey H, Mulhaupt R. Macromolecules 1997;30(10):2818.
[22] Li GZ, Wang L, Toghiani H, Pittman Jr. CU, Daulton TL, Koyama K. Macromolecules 2002;34(25):8686.
[23] Li GZ, Shi LH, Chinese J Polym Sci 1999;1791:37.